HHS Public Access

Author manuscript

Heart Rhythm. Author manuscript; available in PMC 2021 July 07.

Published in final edited form as:

Heart Rhythm. 2018 November ; 15(11): 1617–1625. doi:10.1016/j.hrthm.2018.05.031.

The Field of View of Mapping Catheters Quantified by Electrogram Associations with Radius of Myocardial Attenuation on Contrast-Enhanced Cardiac Computed Tomography

Satish Misra, MD, **Sohail Zahid, BS**[§], **Adityo Prakosa, PhD**[§], **Nissi Saju, RN**[*], **Hari Tandri, MD**[*], **Ronald D. Berger, MD, PhD**[*], **Joseph E. Marine, MD**[*], **Hugh Calkins, MD**[*], **Vadim Zipunnikov, PhD**[§§], **Natalia Trayanova, PhD**[§], **Stefan L. Zimmerman, MD**[**], **Saman Nazarian, MD, PhD**[***]

[*]Department of Cardiology, The Johns Hopkins University School of Medicine, Baltimore, MD [**]Department of Radiology, The Johns Hopkins University School of Medicine, Baltimore, MD [***]Department of Cardiology, University of Pennsylvania, Philadelphia, PA [§]Department of Biomedical Engineering, The Johns Hopkins University, Baltimore, MD [§§]Department of Epidemiology, The Johns Hopkins University School of Public Health, Baltimore, Maryland.

Abstract

Background: Contrast enhanced cardiac computed tomography (CE-CT) provides useful substrate characterization in patients with ventricular tachycardia (VT).

Objective: To describe the association between endocardial electrogram measurements and myocardial characteristics on CE-CT, in particular the field of view of electrogram features.

Methods: Fifteen patients with post-infarct VT who underwent catheter ablation with pre-procedural CE-CT were included. Electroanatomic maps were registered to CE-CT and myocardial attenuation surrounding each endocardial point was measured at radii of 5, 10, and 15 mm. The association between endocardial voltage and attenuation was assessed using a multi-level random effects linear regression model, clustered by patient, with best model fit defined by highest log likelihood (LL).

Results: A total of 4,698 points were included. There was a significant association between bipolar and unipolar voltage with myocardial attenuation at all radii. For unipolar voltage, the best model fit was at an analysis radius of 15 mm regardless of mapping catheter used. For bipolar voltage, the best model fit was at an analysis radius of 15 mm for points acquired with a conventional ablation catheter. In contrast, the best model fit for points acquired with a multipolar mapping catheter was at an analysis radius of 5 mm.

Corresponding Author: Satish Misra, MD, Johns Hopkins University School of Medicine, Division of Cardiology, 1800 Orleans St/ Zayed 7125, Baltimore, MD 21287, smisra5@jhmi.edu.

Conclusion: Myocardial attenuation on CE-CT indicates a smaller myocardial field of view of bipolar electrograms using multipolar catheters with smaller electrodes in comparison to standard ablation catheters despite similar inter-electrode spacing. Smaller electrodes may provide improved spatial resolution for definition of myocardial substrate for VT ablation.

Keywords

Ventricular tachycardia; ventricular arrhythmia; catheter ablation; cardiac computed tomography; Electroanatomic mapping

Introduction

Catheter ablation has been shown to reduce the risk of recurrent ventricular tachycardia (VT).[1–4] In patients with monomorphic VT, the most common mechanism is reentry mediated by slow conduction through heterogeneous scar tissue.[5–7]

Prior studies have shown that scar identified by cardiac magnetic resonance imaging (cMRI) is associated with increased risk of ventricular arrhythmia as well as with areas of low voltage, fractionation, late potentials, and critical isthmus sites.[8–12] The use of contrast enhanced computed tomography (CE-CT) for substrate characterization has also been explored.[13–15] Characteristics including wall thinning, first-pass segmental perfusion, delayed enhancement, adipose tissue deposition, and wall motion abnormalities have also been shown to be associated with endocardial low voltage, presence of abnormal electrograms, and critical isthmus sites.[10,16–18]

In this study, we investigated the association between endocardial electrogram characteristics and myocardial attenuation on CE-CT in patients with post-infarct ventricular tachycardia (PI-VT). We further sought to characterize the myocardial field of view of endocardial voltage through a quantitative analysis of the myocardium surrounding each endocardial point.

Methods

Patient Selection

Patients with a history of PI-VT who underwent VT ablation at a single tertiary care center between 2010 and 2016 with pre-procedural CE-CT, for which raw data files were available to facilitate appropriate reconstruction, were considered eligible for this study. Patients were enrolled with a goal of including 5,000 points for analysis. The study protocol was approved by the Johns Hopkins Institutional Review Board.

Pre-Procedural Cardiac Imaging

CE-CT was acquired using a Toshiba Aquillion 320-slice MDCT scanner with the following parameters: prospective ECG gating (mid-diastole), bolus triggered based on descending aorta attenuation, FOV 200 mm, range 140 mm, gantry rotation 0.275 ms, tube voltage 100–120 kV, tube current 310–700 mA, target HR 60 bpm. Contrast (Isovue-370 in 14, Visipaque in 1; 70–80 cc) was administered as (1) contrast injection (2) 50/50 contrast/saline injection

and (3) saline flush. Images were reconstructed using myocardium-optimized reconstruction kernels including beam hardening artifact correction (thickness 0.5 – 1 mm). The epicardium and endocardium were contoured using semi-automatic segmentation with the open source imaging segmentation software ITK-SNAP (http://www.itksnap.org).[19] A surface mesh of the myocardium ("myocardial mesh"), the volume between the endocardial and epicardial contours, was generated (Figure 1). Artifact, defined as high attenuation (>500 HU) regions surrounding intracardiac leads or calcification as well as associated streaking/shadowing, was manually labeled.

Electroanatomic Mapping

Electroanatomic mapping ("EAM mesh") of the LV was performed with CARTO 3 using either a PentaRay multipolar catheter or Thermocool ablation catheter (Biosense Webster, Diamond Bar, CA) and registered to a CT-derived LV mesh ("CARTO CT mesh") using landmark followed by surface registration. The PentaRay catheter available at our institution has 1 mm electrode size with 4 electrodes per spline with inter-electrode spacing of 4 mm. Bipolar electrograms were recorded between adjacent electrodes with two bipoles per spline (e.g. 1,2 and 3,4). The Thermocool ablation catheter has a 3.5 mm tip electrode and a 2 mm proximal electrode with an inter-electrode spacing of 2 mm.

Bipolar and unipolar electrograms were filtered at 10 to 400 Hz and 1 to 240 Hz, respectively, and recorded as the difference between the highest and lowest deflections of a stable contact signal. Electrogram duration was manually measured from the onset to the end of electrogram deflections at 400 mm/s speed. In accepting the electrogram at each EAM point, we confirmed that ≥2 consecutive electrograms had the same morphology to avoid electrogram artifact due to poor catheter contact.

VT Substrate Identification and Catheter Ablation

Scar was delineated via bipolar voltage mapping (scar < 0.5 mV; border zone 0.5 mV – 1.5 mV; normal >1.5 mV). Fractionated and isolated potentials within and at the periphery of scar were tagged. For hemodynamically stable VT, sites were interrogated using entrainment techniques to assess participation in VT circuits. For hemodynamically unstable VT, pace mapping was utilized from sites with abnormal electrograms to estimate the participation of such sites in VT circuits. Sites that were demonstrated to participate in VT circuits were ablated using an irrigated RF catheter (Thermocool, Biosense Webster) with up to 50 Watts for 60 seconds per lesion or until lack of capture at 10 mA. Additional ablation lesions were delivered to sites of abnormal electrograms at operator discretion.

Registration of CT and Electroanatomic Map

The myocardial mesh, EAM mesh, and CARTO CT mesh were loaded to Slicer3D (http://www.slicer.org), an open-source medical image informatics software, for registration.[20] Using the registration matrix generated in CARTO3, the CARTO CT mesh was registered to the EAM mesh and both subsequently registered to the myocardial mesh (Figure 1). A transformation matrix based on this registration was then derived for conversion of CARTO point coordinates into CT coordinates. The surface registration error was calculated by

measuring the distance between the mapped EAM surface and the myocardial mesh using MATLAB (MathWorks, Natick, Massachusetts).

Using Fiji (http://www.imagej.net/Fiji), the myocardium was isolated from the CE-CT by using a layer mask derived from the myocardial mesh (Figure 1). [24] Text files containing the voxel coordinates, attenuation, and labels were generated. The average attenuation of all voxels within a radius (5 mm, 10 mm, 15 mm in the X, Y, Z axis) of the nearest myocardial point to the EAM point was measured using MATLAB (Figure 1).[21] Calcification or lead artifact related high-attenuation signals are expected to have a reverse association with electrogram characteristics in comparison to other areas of myocardium. Since this analysis used a linear framework, EAM points that were in these areas of myocardium were excluded.

Statistical Analysis

Statistical analysis was performed using STATA version 12 (StataCorp, College Station, Texas). Multi-level random effects linear regression models, clustered by patient, were used to characterize the correlation between myocardial attenuation, endocardial bipolar voltage, unipolar voltage, and electrogram duration. Voltage was log transformed to adjust for skew. The adjusted model included the gender, body mass index (BMI), and ejection fraction (EF) consistent with prior studies. Gender was included due to associated variation in myocardial mass. BMI was included due to the potential impact of increased extra-cardiac tissue on attenuation despite adjustments to mitigate those differences. EF was included as differences in the degree of cardiomyopathy may have several potential impacts on cardiac CT. The best model fit was defined as the analysis radius at which the log likelihood (LL) was greatest.

Results

Baseline Characteristics

Fifteen patients were included in this study (Table 1). Fourteen patients had an ICD (single chamber: 4; dual chamber: 6, CRT-D: 4). Fourteen patients were mapped in sinus rhythm; one pacemaker-dependent patient was mapped in ventricular paced rhythm. Eleven patients were undergoing initial ablation. One patient was non-inducible for VT at baseline and underwent substrate modification. Four patients did not have post-ablation testing due to procedural duration. Among the remaining patients, six were non-inducible for any VT post-ablation and three were non-inducible for the clinical VT (defined by the operator based on 12-lead morphology or intracardiac morphology/cycle length). One remained inducible for the clinical VT. There were no major complications.

Electroanatomic Mapping and CE-CT Imaging

A total of 5,094 points were acquired during baseline rhythm that met electrogram stability criteria. Of these points, 7.8% were excluded due to artifact leaving 4,698 electrograms (82% PentaRay, 18% Thermocool). The median surface registration error was 3.6 mm (interquartile range 1.8 mm – 6.9 mm). Of the analyzed points, 36% were consistent with dense scar, 33% with border zone, and 31% with normal tissue (Figure 2). A prolongation in

the EGM duration was observed across tissue types in both catheter groups ($p < 0.001$ for between group differences, Table 2).

The average myocardial volume affected by artifact was 9% (2% – 21%), excluding the patient without an ICD. Regions of myocardium impacted by artifact varied depending on insertion site of the right ventricular lead (mid-septal, distal septal, or distal RV free wall) and presence of coronary sinus lead (basal lateral LV).

Association of Endocardial Voltage to Local Myocardial Attenuation: Pooled Analysis with both Catheter Types

In unadjusted analysis, there was an association between unipolar voltage and myocardial attenuation at all analysis radii (5, 10, and 15 mm; Table 3). There was also an association between bipolar voltage and myocardial attenuation at analysis radii of 10 mm and 15 mm. The best model fit was at a radius of 15 mm for both bipolar and unipolar voltage (LL —3273.89 and −7265.74 respectively). In the adjusted model, there was an association between both bipolar and unipolar voltage with myocardial attenuation at all analysis radii. In this model, the best model fit was at a radius of 15 mm both for bipolar and unipolar voltage (LL −2024.38 and 4286.47respectively).

Association of Endocardial Voltage to Local Myocardial Attenuation: Stratified Analysis by Catheter Type

For points obtained using a Thermocool ablation catheter, there was a significant association between bipolar voltage and myocardial attenuation at all analysis radii (5, 10, and 15 mm; Table 3). As shown in Table 3, the best model fit was at an analysis radius of 15 mm (LL −1025.31). Similarly, there was a significant association between unipolar voltage and myocardial attenuation at all analysis radii. The best model fit was also at 15 mm (LL -599.17).

When restricting analysis to points obtained using a PentaRay catheter, there was a significant association between bipolar voltage and myocardial attenuation at all analysis radii (5, 10, and 15 mm; Table 3). In contrast to the above described results associated with the ablation catheter, the best model fit was at an analysis radius of 5 mm (LL −3197.54). Significant associations between unipolar voltage and myocardial attenuation were also seen at all analysis radii. However, the best model fit was at an analysis radius of 15 mm (LL −1385.54) as shown in Table 3.

Correlation of Electrogram Duration to Local Myocardial Attenuation

There was an association between EGM duration and myocardial attenuation at an analysis radius of 5mm in the unadjusted analysis that was lost in the adjusted analysis; no association was observed at analysis radii of 10 mm or 15 mm (Table 4). When restricting analysis in the adjusted model to the 3,235 points consistent with border zone and dense scar, however, there was an association between EGM duration and myocardial attenuation at all measured radii with best model fit at an analysis radius of 15 mm (LL −8844.21). In the stratified analysis by catheter, this relationship held true for points obtained using a PentaRay catheter with the best model fit at an analysis radius of 15 mm (LL −6699.20). For

points obtained with a Thermocool catheter, there was no association between electrogram duration and myocardial attenuation at any radius.

Discussion

In this study of patients with ischemic cardiomyopathy undergoing catheter ablation of ventricular tachycardia, there was an association between endocardial electrogram characteristics and CT-derived myocardial attenuation (Figure 3). While unipolar voltage was associated with the largest field of view regardless of catheter type, bipolar voltage was associated with a smaller field of view when acquired with a multipolar catheter with smaller electrodes than with an ablation catheter with larger electrodes. To our knowledge, this study is the first analysis describing the myocardial "field of view" of endocardial voltage measurements acquired with conventional mapping catheters.

These findings are consistent with prior studies showing an association between endocardial electrogram characteristics and myocardial attenuation. In a study using 64-slice MDCT, Tian et al showed that myocardial segments containing areas of hypoperfusion, as identified on visual review, correlated well with areas of low voltage.[16] We and others have previously shown that myocardial attenuation, also assessed using a segmental model, was directly correlated to bipolar and unipolar voltage.[10,18]

In the present study, we found that the bipolar voltage was associated with a smaller field of view when using a multi-electrode catheter with bipoles consisting of 1 mm electrodes separated by 4 mm in comparison to an ablation catheter with a bipole consisting of a tip 3.5 mm electrode and proximal 2 mm electrode separated by 3.5 mm (Figure 4). That the center-to-center interelectrode spacing between these catheters is similar suggests that other factors contribute to difference in the field of view observed. Both smaller electrode size and the angle of incidence of the bipole with the myocardium can affect the underlying tissue diameter and therefore the overall field of view of the bipolar electrogram, though the relative impact is unclear.[22–24] Of note, while areas of hypoattenuation reflecting scar can be visually defined on CE-CT, the differences between catheter type identified in this study were defined through quantitative analysis of myocardial attenuation and may not be discernible on visual analysis by an interpreting physician.

Prior studies have described the improved resolution of electroanatomic maps generated with catheters that have smaller electrodes and inter-electrode spacing, allowing identification of channels of viable myocardium in areas of dense scar that may support reentrant arrhythmia.[22,25] In addition to electrode size and spacing, factors such as the activation wavefront can affect the local electrogram.[22–24] In normal myocardium, the bipolar electrogram can be affected by the direction of the activation wavefront relative to the orientation of the bipole as well as the local fiber orientation. These wavefront-dependent differences in electrogram amplitude and morphology are likely accentuated in diseased myocardium where viable myocardial fibers are interspersed within fibrotic tissue leading to more complex impulse propagation dependent on the direction of activation. In this study, a single activation wavefront was mapped in each patient. However, Tung et al found that the wavefront-dependent variation in endocardial voltage may be more significant

in patients with greater scar heterogeneity or non-ischemic cardiomyopathy. Therefore variations related to activation wavefront may have less effect in the cohort of patients included in the present study.[26]

Additionally, since the bipolar angle for mapping changes at random, there is no reason to suspect geographically differential bias in voltage assessment in the type of analysis performed in this study. Nonetheless, sensitivity analysis by adding rhythm during mapping to the multivariable model revealed no significant changes to the model results or fit.

Interestingly, the association between electrogram duration and attenuation was limited to electrograms obtained using a PentaRay catheter in regions of dense scar and border zone. This finding may reflect the impact of non-uniform conduction in heterogeneous, diseased tissue in this region as well as the effect of electrode size and bipole orientation relative to the myocardium. Overall, the findings of our study further demonstrate that smaller bipole configurations provide a smaller myocardial field of view, in this case reflecting the structural characteristics of a smaller region of myocardium as assessed by cardiac CT.

Cardiac CT does offer some potential advantages in comparison to cMRI for substrate characterization including greater accessibility, excellent spatial resolution, and unique substrate definition opportunities such as simplified delineation of adipose tissue from myocardial fibrosis. That the field of view of endocardial bipolar voltage varies as expected with bipole configuration suggests that cardiac CT has sufficient resolution such that quantitative analysis of myocardial attenuation may offer additional information that could aide in catheter ablation and should be investigated further.

Limitations

There are several limitations that are important to consider. First, various forms of artifact may impact the attenuation, despite mitigation with using reconstruction kernels that included artifact correction. Second, registration error could affect attenuation measurement around each point. However, the smallest radius analyzed was 5 mm whereas the median registration error was 3.6 mm. Third, measurements of endocardial electrograms can be falsely low due to poor catheter contact, which we mitigated with strict electrogram inclusion criteria. Further, endocardial mapping was performed using one catheter in each enrolled patient. While no selection bias was noted regarding catheter selection, it is possible this could introduce unknown confounding factors when making comparisons between the catheters themselves. Additionally, we did not analyze unfiltered unipolar signals. Future prospective studies that compare cardiac CT images to the entire frequency spectrum for unipolar signals as well as comparison to endocardial mapping with different catheter types in the same patient would be of considerable interest. Finally, the use of AADs may effect the measured endocardial voltage; as most patients were on AADs, it is unclear what affect, if any, this factor would have on the overall associations of voltage and attenuation.

Conclusion

Myocardial attenuation on CE-CT is associated with endocardial bipolar and unipolar voltage measurements. For bipolar voltage measurements, a multi-electrode mapping

catheter with smaller electrode size was associated with a 5 mm field of view in comparison to a 15 mm field of view for a standard ablation catheter with larger electrodes despite similar interelectrode spacing. Use of electrode mapping catheters with smaller electrodes may provide better definition of myocardial substrate for VT ablation.

Acknowledgments

Disclosures: Dr. Nazarian is a consultant for St Jude Medical, Siemens, Biosense Webster, and CardioSolv. Dr. Nazarian serves as PI for research funding from Biosense Webster. The University of Pennsylvania Conflict of Interest Committee manages all commercial arrangements.

Funding: The study was funded through NIH grant R01HL116280 to Dr. Nazarian. The contents do not necessarily represent the views of the National Institutes of Health.

References

1. Kuck KH, Schaumann A, Eckardt L, Willems S, Ventura R, Delacretaz E, Pitschner HF, Kautzner J, Schumacher B, Hansen PS. Catheter ablation of stable ventricular tachycardia before defibrillator implantation in patients with coronary heart disease (VTACH): a multicentre randomised controlled trial. Lancet (London, England). 2010;375(9708):31–40.
2. Mallidi J, Nadkarni GN, Berger RD, Calkins H, Nazarian S. Meta-analysis of catheter ablation as an adjunct to medical therapy for treatment of ventricular tachycardia in patients with structural heart disease. Heart Rhythm. 2011;8(4):503–510. [PubMed: 21147263]
3. Reddy VY, Reynolds MR, Neuzil P, Richardson AW, Taborsky M, Jongnarangsin K, Kralovec S, Sediva L, Ruskin JN, Josephson ME. Prophylactic catheter ablation for the prevention of defibrillator therapy. The New England journal of medicine. 2007;357(26):2657–2665. [PubMed: 18160685]
4. Stevenson WG, Wilber DJ, Natale A, et al. Irrigated radiofrequency catheter ablation guided by electroanatomic mapping for recurrent ventricular tachycardia after myocardial infarction: the multicenter thermocool ventricular tachycardia ablation trial. Circulation. 2008;118(25):2773–2782. [PubMed: 19064682]
5. Stevenson WG, Friedman PL, Sager PT, Saxon LA, Kocovic D, Harada T, Wiener I, Khan H. Exploring postinfarction reentrant ventricular tachycardia with entrainment mapping. J Am Coll Cardiol. 1997;29(6):1180–1189. [PubMed: 9137211]
6. Stevenson WG, Khan H, Sager P, Saxon LA, Middlekauff HR, Natterson PD, Wiener I. Identification of reentry circuit sites during catheter mapping and radiofrequency ablation of ventricular tachycardia late after myocardial infarction. Circulation. 1993;88(4 Pt 1):1647–1670. [PubMed: 8403311]
7. Hadjis TA, Stevenson WG, Harada T, Friedman PL, Sager P, Saxon LA. Preferential locations for critical reentry circuit sites causing ventricular tachycardia after inferior wall myocardial infarction. J Cardiovasc Electrophysiol. 1997;8(4):363–370. [PubMed: 9106421]
8. Bello D, Fieno DS, Kim RJ, Pereles FS, Passman R, Song G, Kadish AH, Goldberger JJ. Infarct morphology identifies patients with substrate for sustained ventricular tachycardia. J Am Coll Cardiol. 2005;45(7):1104–1108. [PubMed: 15808771]
9. Nazarian S, Bluemke DA, Lardo AC, et al. Magnetic resonance assessment of the substrate for inducible ventricular tachycardia in nonischemic cardiomyopathy. Circulation. 2005;112(18):2821–2825. [PubMed: 16267255]
10. Sasaki T, Calkins H, Miller CF, Zviman MM, Zipunnikov V, Arai T, Sawabe M, Terashima M, Marine JE, Berger RD, Nazarian S, Zimmerman SL. New insight into scar-related ventricular tachycardia circuits in ischemic cardiomyopathy: Fat deposition after myocardial infarction on computed tomography--A pilot study. Heart Rhythm. 2015;12(7):1508–1518. [PubMed: 25814415]

11. Sasaki T, Miller CF, Hansford R, et al. Myocardial structural associations with local electrograms: a study of postinfarct ventricular tachycardia pathophysiology and magnetic resonance-based noninvasive mapping. Circ Arrhythm Electrophysiol. 2012;5(6):1081–1090. [PubMed: 23149263]
12. Sasaki T, Miller CF, Hansford R, et al. Impact of nonischemic scar features on local ventricular electrograms and scar-related ventricular tachycardia circuits in patients with nonischemic cardiomyopathy. Circ Arrhythm Electrophysiol. 2013;6(6):1139–1147. [PubMed: 24235267]
13. Lardo AC, Cordeiro MA, Silva C, et al. Contrast-enhanced multidetector computed tomography viability imaging after myocardial infarction: characterization of myocyte death, microvascular obstruction, and chronic scar. Circulation. 2006;113(3):394–404. [PubMed: 16432071]
14. Zafar HM, Litt HI, Torigian DA. CT imaging features and frequency of left ventricular myocardial fat in patients with CT findings of chronic left ventricular myocardial infarction. Clinical radiology. 2008;63(3):256–262. [PubMed: 18275865]
15. Gupta M, Kadakia J, Hacioglu Y, Ahmadi N, Patel A, Choi T, Yamada G, Budoff M. Non-contrast cardiac computed tomography can accurately detect chronic myocardial infarction: Validation study. Journal of nuclear cardiology : official publication of the American Society of Nuclear Cardiology. 2011;18(1):96–103. [PubMed: 21128040]
16. Tian J, Jeudy J, Smith MF, et al. Three-dimensional contrast-enhanced multidetector CT for anatomic, dynamic, and perfusion characterization of abnormal myocardium to guide ventricular tachycardia ablations. Circ Arrhythm Electrophysiol. 2010;3(5):496–504. [PubMed: 20657032]
17. Komatsu Y, Cochet H, Jadidi A, et al. Regional myocardial wall thinning at multidetector computed tomography correlates to arrhythmogenic substrate in postinfarction ventricular tachycardia: assessment of structural and electrical substrate. Circ Arrhythm Electrophysiol. 2013;6(2):342–350. [PubMed: 23476043]
18. Esposito A, Palmisano A, Antunes S, Maccabelli G, Colantoni C, Rancoita PM, Baratto F, Di Serio C, Rizzo G, De Cobelli F, Della Bella P, Del Maschio A. Cardiac CT With Delayed Enhancement in the Characterization of Ventricular Tachycardia Structural Substrate: Relationship Between CT-Segmented Scar and Electro-Anatomic Mapping. JACC Cardiovascular imaging. 2016;9(7):822–832. [PubMed: 26897692]
19. Yushkevich PA, Piven J, Hazlett HC, Smith RG, Ho S, Gee JC, Gerig G. User-guided 3D active contour segmentation of anatomical structures: significantly improved efficiency and reliability. NeuroImage. 2006;31(3):1116–1128. [PubMed: 16545965]
20. Fedorov A, Beichel R, Kalpathy-Cramer J, et al. 3D Slicer as an image computing platform for the Quantitative Imaging Network. Magnetic resonance imaging. 2012;30(9):1323–1341. [PubMed: 22770690]
21. Schindelin J, Arganda-Carreras I, Frise E, et al. Fiji: an open-source platform for biological-image analysis. Nature methods. 2012;9(7):676–682. [PubMed: 22743772]
22. Anter E, Tschabrunn CM, Buxton AE, Josephson ME. High-Resolution Mapping of Postinfarction Reentrant Ventricular Tachycardia: Electrophysiological Characterization of the Circuit. Circulation. 2016;134(4):314–327. [PubMed: 27440005]
23. Anter E, Tschabrunn CM, Josephson ME. High-resolution mapping of scar-related atrial arrhythmias using smaller electrodes with closer interelectrode spacing. Circ Arrhythm Electrophysiol. 2015;8(3):537–545. [PubMed: 25792508]
24. Stevenson WG, Soejima K. Recording techniques for clinical electrophysiology. J Cardiovasc Electrophysiol. 2005;16(9):1017–1022. [PubMed: 16174026]
25. Tschabrunn CM, Roujol S, Dorman NC, Nezafat R, Josephson ME, Anter E. High-Resolution Mapping of Ventricular Scar: Comparison Between Single and Multielectrode Catheters. Circ Arrhythm Electrophysiol. 2016;9(6).
26. Tung R, Josephson ME, Bradfield JS, Shivkumar K. Directional Influences of Ventricular Activation on Myocardial Scar Characterization: Voltage Mapping With Multiple Wavefronts During Ventricular Tachycardia Ablation. Circ Arrhythm Electrophysiol. 2016;9(8).

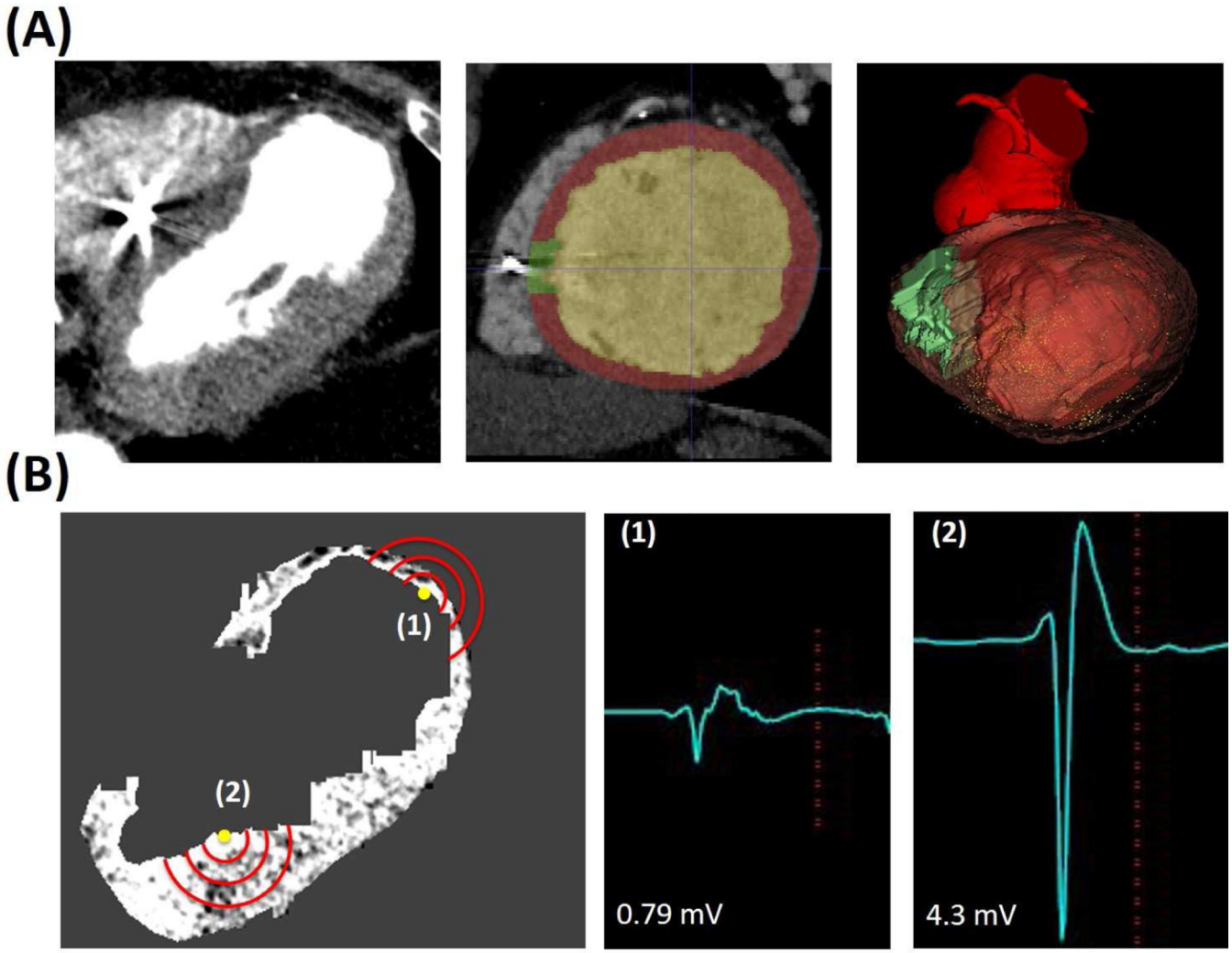

Figure 1: Registration of CE-CT to Electroanatomic Map and Field of View Analysis

Panel A: CE-CT Segmentation with isolation of ICD lead artifact for exclusion in subsequent analysis and generation of myocardial mesh. Left image shows CE-CT, middle image shows representative segmentation (green = artifact, red = myocardium, yellow = blood pool), and right image shows resulting myocardial model registered to the electroanatomic map (yellow dots indicate mapping points). Panel B: Representative image showing co-registered EAM points on CE-CT with different analysis radii (red lines) and associated electrograms.

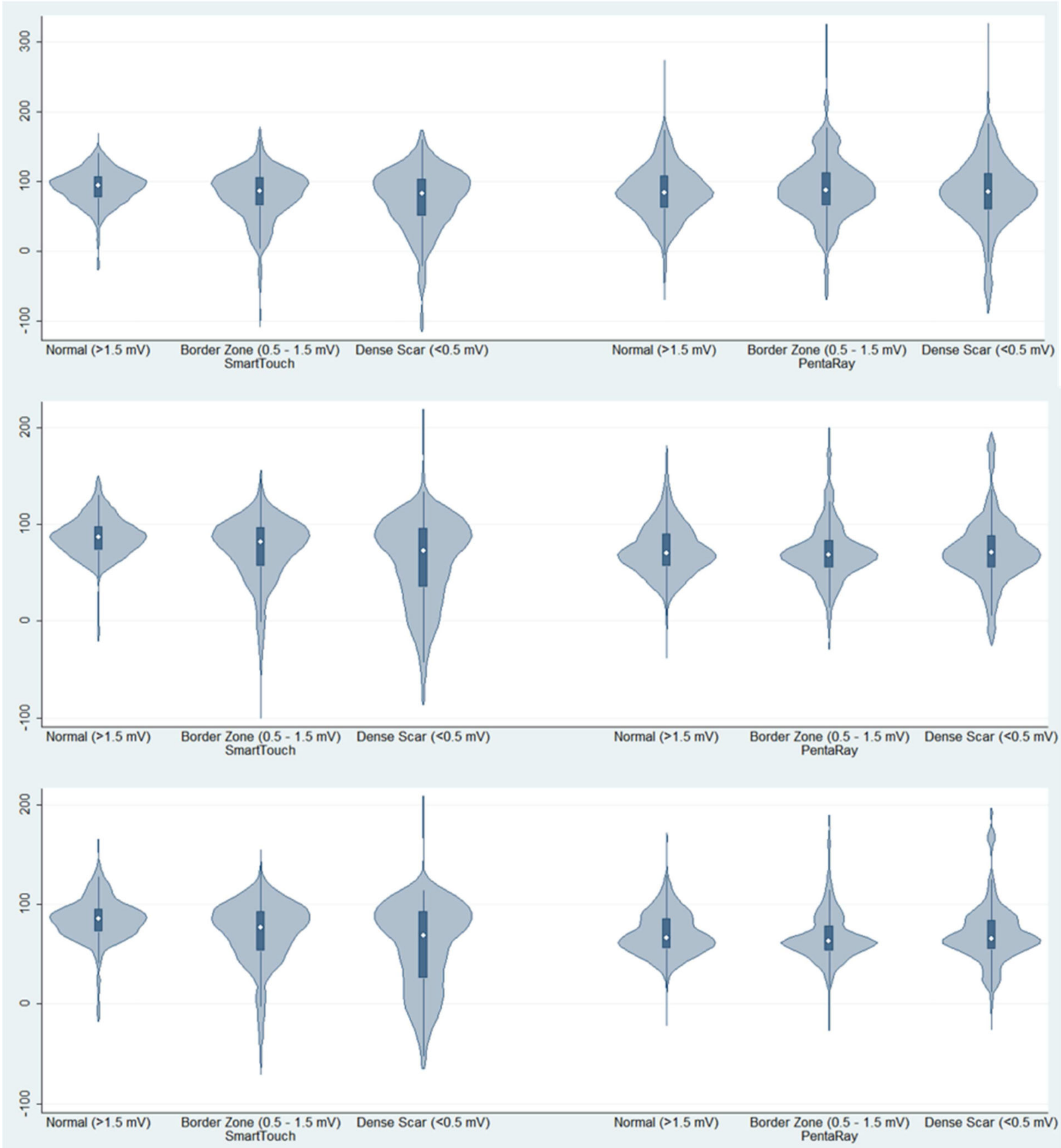

Figure 2: Distribution of Myocardial Attenuation in Scar, Border Zone, and Normal Tissue by Catheter Type

Violin plots showing distribution of myocardial attenuation (HU; y-axis) is show by tissue type (scar, border zone, normal as defined by endocardial bipolar voltage) and grouped by catheter type.

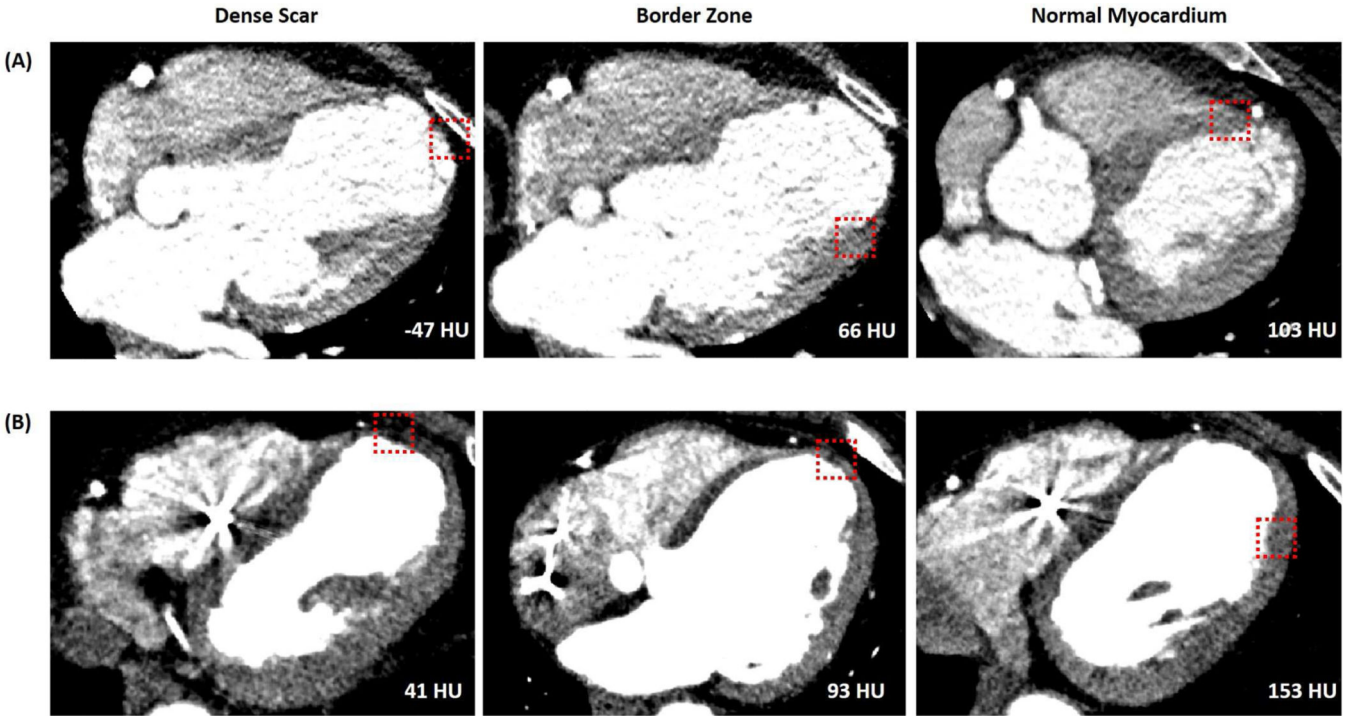

Figure 3: Examples of Myocardial Characteristics on CE-CT at Scar, Border Zone, and Normal Myocardium

Examples of myocardial characteristics on CE-CT at scar, border zone, and normal myocardium (left to right) as defined by endocardial voltage. (Panel A) Patient in whom mapping was performed with a Thermocool ablation catheter. (Panel B) Patient in whom mapping was performed using a PentaRay. Red box highlights location of electroanatomic mapping point and the associated attenuation at an analysis radius of 5 mm is shown on each image.

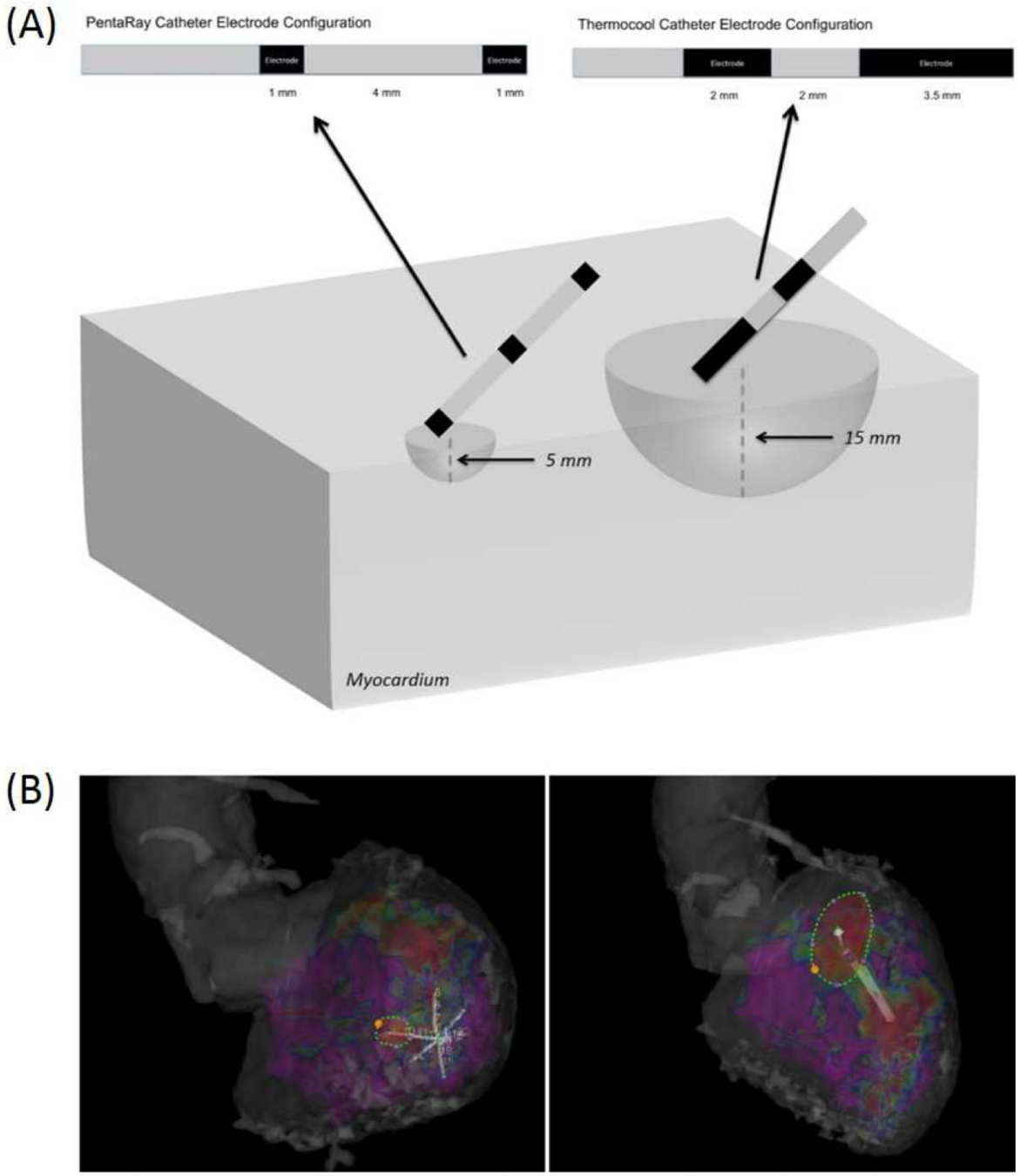

Figure 4: Optimal Field of View of Endocardial Bipolar Voltage Based on the Catheter Type and Associated Electrode Configuration

(A) Schematic of electrode configurations of catheters used during endocardial substrate mapping with associated optimal field of view (hemisphere) based on association with local myocardial attenuation. (B) Electroanatomic mapping showing PentaRay catheter (left) and Thermocool catheter (right) with the endocardial surface area associated with 5 mm and 15 mm field of view respectively.

Table 1:

Baseline Characteristics

	All Patients	PentaRay Group[3]	Thermocool Group[3]
Number	15	7	8
Age (years)[1]	60 (50–70)	70 (59–74)	54 (46–63)
Gender (n)[2]			
Male	11 (73%)	5 (71%)	6 (75%)
Female	4 (27%)	2 (29%)	2 (25%)
Ejection Fraction (%)[1]	32.5% (17.5–42.5%)	32.5 (12.5–42.5)	22.5 (17.5–47.5)
Anti-arrhythmic Use (n)[2]	14 (93%)	7 (100%)	7 (88%)
Class I	4 (27%)	3 (42%)	1 (13%)
Class III	12 (80%)	5 (71%)	7 (88%)
VT inducible at baseline (%)[2]	14 (93%)	6 (86%)	8 (100%)
Clinical VT non-inducible post-ablation (%)[2,4]	9 (64%)	4 (67%)	5 (63%)
Total Points Acquired[1]	151 (84–364)	364 (283 – 579)	88 (56–102)

[1]Continuous variables are reported as median (interquartile range)

[2]Categorical variables are reported with absolute values and percentages.

[3]Catheter groups are based on the primary catheter used for substrate mapping prior to ablation.

[4]One patient non-inducible at baseline, 4 patients not tested post ablation (2 Thermocool, 2 PentaRay).

Table 2:

Electrogram Characteristics within Scar, Border Zone, and Normal Myocardium

	Dense Scar	Border Zone	Normal Myocardium
Thermocool			
Bipolar Voltage (mV)	0.30 (0.04 – 0.498)	0.93 (0.501 – 1.49)	3.6 (1.5 – 14.8)
Unipolar Voltage (mV)	3.09 (0.93 – 7.63)	4.5 mV (1.18 – 11.3)	8.2 (2.6 – 23.5)
EGM Duration (ms)	146 (64–232)	137 (74–235)	118 (48–231)
PentaRay			
Bipolar Voltage (mV)	0.27 (0.036 – 0.498)	0.85 (0.501 – 1.497)	4.42 (1.5 – 29.3)
Unipolar Voltage (mV)	4.13 (0.73 – 12.38)	5.50 (0.85 – 14.07)	8.87 (1.61 – 31.22)
EGM Duration (ms)	147 (56–268)	134 (71–228)	120 (57–280)

Values are shown as mean and 95% confidence interval. P<0.001 for between group differences (scar, border zone, normal myocardium) for each characteristic.

Table 3:

Association of Endocardial Voltage with Myocardial Attenuation at Varying Radii

	5mm	10mm	15mm
All Points Unadjusted Analysis			
Bipolar Voltage	0.01 (−0.08, 0.09; p = 0.844)	0.31 (0.19; 0.42; p < 0.001)	0.48 (0.34, 0.61; p < 0.001)
Unipolar Voltage	0.11 (0.07, 0.14; p < 0.001)	0.27 (0.22, 0.32; p < 0.001)	0.35 (0.29, 0.41; p < 0.001)
All Points Adjusted Analysis			
Bipolar Voltage	0.43 (0.32, 0.54; p < 0.001)	0.62 (0.47, 0.76; p < 0.001)	0.69 (0.53, 0.85; p < 0.001)
Unipolar Voltage	0.28 (0.23, 0.33; p < 0.001)	0.46 (0.40, 0.53; p < 0.001)	0.55 (0.48, 0.62; p < 0.001)
Thermocool Ablation Catheter			
Bipolar Voltage	0.50 (0.28, 0.55; p < 0.001)	0.79 (0.58, 1.01; p < 0.001)	0.95 (0.72, 1.17, p < 0.001)
Unipolar Voltage	0.52 (0.40, 0.63; p < 0.001)	0.65 (0.52, 0.77; p < 0.001)	0.72 (0.59, 0.85; p < 0.001)
PentaRay Catheter			
Bipolar Voltage	0.41 (0.28, 0.55; p < 0.001)	0.54 (0.35, 0.72; p < 0.001)	0.55 (0.34, 0.76; p < 0.001)
Unipolar Voltage	0.23 (0.18, 0.28; p < 0.001)	0.39 (0.31, 0.46; p < 0.001)	0.46 (0.38, 0.54; p < 0.001)

Coefficient of association in multilevel random effects regression model presented with 95% confidence interval and p-value. Best model fit identified by grey shading.

Table 4:

Association of Electrogram Duration with Myocardial Attenuation at Varying Radii by Catheter Type

	5mm	10mm	15mm
All Points (unadjusted)	2.27 (0.39, 4.14; p = 0.02)	−0.72 (−3.42, 1.99; p = 0.60)	−1.17 (−4.45, 2.11; p = 0.49)
All Points (adjusted)	0.57 (−2.09, 3.34; p = 0.67)	0.49 (−3.14, 4.11; p = 0.79)	1.45 (−2.71, 5.61; p = 0.49)
Normal Myocardium	5.68 (0.23, 11.14, p = 0.04)	5.82 (−1.19, 12.82, p = 0.10)	7.11 (−0.72, 14.95, p = 0.08)
Scar and Border Zone	3.47 (0.99, 5.94, p = 0.006)	4.38 (1.14, 7.62, p = 0.008)	5.77(2.11, 9.43, p = 0.002)
PentaRay (Scar/BZ)	3.54 (0.78 – 6.30, p = 0.012)	4.83 (1.05 – 8.61, p = 0.012)	6.42 (2.06 – 10.78, p = 0.004)
Thermocool (Scar/BZ)	2.61 (−3.09, 8.30, p = 0.37)	3.06 (−3.28, 9.39, p = 0.345)	4.77 (−2.08, 11.62, p = 0.173)

Coefficient of association in multilevel random effects regression model presented with 95% confidence interval and p-value. Best model fit identified by grey shading.